azide binding (Figure 1). In the present structure the side chain of Arg-145 has extended toward the interior of the active site cavity by 0.7 Å and the plane of the guanidinium group is rotated in a position almost perpendicular with respect to its orientation in the native enzyme. The L-phe binding to the enzyme is not prevented by this new conformation, but it is actually favored. In fact the new position of the Arg-145 side chain makes possible a closer approach of the L-phe amino nitrogen to the carboxylate group of Glu-270. On the contrary, the binding of a polypeptide substrate can be hindered because once the terminal carboxylate is bound to the rotated Arg-145, the peptide link is not pointing any longer toward the S1 catalytic site, but it is pushed toward the cavity wall.

The second azide binding site can be tentatively assigned to the zinc ion. As already noted, this density is lower than that on Arg-145 (3.0–3.5σ), but its shape is very similar (Figure 2). It must be stressed again that electron density corresponding to disordered solvent will always be indistinguishable from that of the azide ion. This observation, together with the fact that the structure was determined with a limited amount of observed reflections, suggests great caution in the above interpretation. Our interpretation is consistent with the proposed model of activation of the zinc-bound water molecule toward anion substitution.[4,12] The low-affinity-site model is also consistent with the spectroscopic observations of a charge transfer between a cobalt-bound azide ion and the metal in the corresponding ternary complex with CoCPA.[12]

The synergism in the azide and the L-phe binding to CPA is explained by the presence of the azide molecule on the high-affinity site near Arg-145 which forces its guanidinium group to adopt the extended conformation described above (Figure 1). This new conformation allows the simultaneous near-optimal interactions of L-phe both with Arg-145 and with Glu-270 which would be otherways mutually exclusive as observed in the other L-phe-containing complexes[16,17] (vide supra). It is interesting to point out that due to the different chirality of the α carbon, the D-phe amino acid can also perform such simultaneous hydrogen bonds.[15] On the other hand, the interaction of L-phe with Glu-270 weakens the hydrogen bond between Glu-270 and the metal-bound water molecule, favoring its replacement by the second azide ion. Further stabilization of the ternary complex can be achieved by the network of hydrogen bonds and electrostatic interactions which link the L-phe molecule to the metal-bound azide anion through the bridging Glu-270 carboxylate and the stabilization of low-affinity azide by contacts with Ser-197 and water molecules bound in the cavity.

Acknowledgment. We are grateful to Dr. David W. Christianson for continuous advice and suggestions and to Professor Ivano Bertini and all the researchers of the Bioinorganic Laboratory of the University of Florence for stimulating discussions and comments. The use of the Philips PW1100 diffractometer of the ISSECC (Florence, Italy) is gratefully acknowledged.

Registry No. CPA, 11075-17-5; Zn, 7440-66-6.

Contribution from the Department of Chemistry, University of California, Berkeley, California 94720

Synthesis, Structure, and Properties of $[Mn(salpn)(EtOH)_2](ClO_4)$ and Its Aerobic Oxidation Product $[Mn(salpn)O]_2$[1]

Joel W. Gohdes and William H. Armstrong*

Received August 17, 1990

Preparation and isolation of the mononuclear Mn^{III} complex $[Mn(salpn)(EtOH)_2](ClO_4)$ (**1a**) (H_2salpn = *N,N'*-bis(salicylidene)-1,3-diaminopropane) were accomplished by air oxidation of a solution containing H_2salpn, NaOH, and $Mn(ClO_4)_2 \cdot 6H_2O$ in MeOH/EtOH (1:1), followed by addition of Et_2O. Compound **1a**·EtOH·H_2O crystallizes in the triclinic space group $P\bar{1}$ with a = 11.649 (3) Å, b = 13.902 (6) Å, c = 19.849 (7) Å, α = 70.18 (2)°, β = 70.52 (2)°, γ = 60.33 (2)°, V = 2726 (2) Å^3, and Z = 4. For **1a**·EtOH·H_2O there are two mononuclear Mn^{III} complexes in the crystallographic asymmetric unit. The Mn–O and Mn–N distances for **1** are in good agreement with those found for other Mn^{III} Schiff base complexes. The ^{1}H NMR spectrum of **1** in CD_3CN has well-resolved, paramagnetically shifted resonances at 19.8, 11.6, 7.4, −2.8, −24.8, −26.2, and −94.2 ppm. Compound **1** has a $Mn^{III/II}$ reduction potential of −0.154 V vs SSCE as measured by cyclic voltammetry in DMSO. Compound **1** was converted into $[Mn_2O_2(salpn)_2]$ (**2**) by air oxidation in basic MeOH followed by recrystallization from DMF. Alternatively, **2** can be prepared by air oxidation of $Mn(salpn)(H_2O)$ in pyridine, followed by crystallization from CH_2Cl_2/cyclohexane. Compound **2**·2DMF crystallizes in the monoclinic space group $P2_1/c$ with a = 10.722 (2) Å, b = 10.163 (3) Å, c = 17.564 (4) Å, β = 100.67 (2)°, V = 1890 (1) Å^3, and Z = 2. Using an isotropic spin-exchange Hamiltonian $\mathcal{H} = -2J\hat{S}_1 \cdot \hat{S}_2$, variable-temperature magnetic data for **2** were fit well with a J value of −82 cm^{-1}. The magnitude of J is significantly less than that for several other species containing the $\{Mn_2O_2\}^{4+}$ core yet comparable to the value obtained for $[Mn_2O_2(pic)_2]$ (pic = 2-pyridinecarboxylate) (*Inorg. Chem.* **1989**, *28*, 4037). The reduction potential for **2** in DMSO (−0.39 V vs SSCE) for the IV,IV/IV,III couple is the lowest determined for a bis(μ-oxo)dimanganese complex.

Manganese plays an important role in several biological redox-active systems. In three of these systems—the oxygen-evolving complex in photosystem II of green plants,[2] Mn catalases,[3] and Mn ribonucleotide reductase[4]—the active sites are thought to exist as binuclear species or manganese aggregates of higher nuclearity. Because these metalloenzymes function as multielectron-redox catalysts, it is reasonable to assume that the manganese sites serve as reservoirs of reducing or oxidizing equivalents. The accessibility of at least two oxidation states for most manganese coordination complexes makes it a suitable metal for this function. The most extensively studied of the biological systems has been the photosystem II oxygen-evolving complex (PSII OEC). Although it is known that there are four manganese atoms per OEC,[5] the precise arrangement of these four atoms has not been determined unambiguously.[6] EXAFS analysis of the OEC indicates the

(1) Abbreviations used: salpn = *N,N'*-bis(salicylidene)-1,3-diaminopropane; EtOH = ethanol; EXAFS = extended X-ray absorption fine structure; PSII OEC = photosystem II oxygen-evolving complex; phen = phenanthroline; bispicen = *N,N'*-bis(2-pyridylmethyl)-1,2-ethanediamine; pic = 2-pyridinecarboxylate; DMF = *N,N*-dimethylformamide.

(2) (a) Brudvig, G. W. In *Metal Clusters in Proteins*; Que, L., Jr., Ed.; ACS Symposium Series 372; American Chemical Society: Washington, DC, 1988; pp 221–237. (b) Babcock, G. T. In *New Comprehensive Biochemistry: Photosynthesis*; Amesz, J., Ed.; Elsevier: Amsterdam, 1987; pp 125–158. (c) Dismukes, G. *Photochem. Photobiol.* **1985**, *42*, 187.

(3) (a) Fronko, R. M.; Penner-Hahn, J. E.; Bender, C. J. *J. Am. Chem. Soc.* **1988**, *110*, 7554. (b) Allgood, G. S.; Perry, J. *J. Bacteriol.* **1986**, *168*, 563. (c) Beyer, W. F., Jr.; Fridovich, I. *Manganese in Metabolism and Enzyme Function*; Academic Press: New York, 1986; p 193.

(4) Willing, A.; Follman, H.; Auling, G. *Eur. J. Biochem.* **1988**, *170*, 603.

(5) Cheniae, G. M.; Martin, I. F. *Biochim. Biophys. Acta* **1970**, *197*, 219.

(6) Pecoraro, V. L. *Photochem. Photobiol.* **1988**, *48*, 249 and references therein.

0020-1669/92/1331-0368$03.00/0

presence of at least one and possibly two or more short (~2.7 Å) Mn···Mn distances.[7] This close contact, consistent with a bis(μ-oxo)dimanganese core, suggests a strong interaction between the manganese atoms involved in this substructure. In order to understand the interaction between manganese atoms within this core type, it is important to study a number of model complexes with a wide range of ligand environments.

Schiff base ligands offer straightforward synthetic access to a variety of ligand environments with biologically relevant donors. Recently, we reported a single-oxo-bridged dimanganese(III) complex of a pentadentate Schiff base ligand.[8] Our interest in manganese coordination chemistry of the Schiff base ligand salpn is based in part on two separate reports in the literature. The first was the report of reversible dioxygen binding by Mn(salpn)(H$_2$O)[9] and the identification of the decomposition product of the proposed dioxygen adduct in pyridine as a Mn(IV) bis(oxo)-bridged dimer.[10] A subsequent crystallographic study of this oxidation product resulted in its being assigned as a Mn^{III} bis(hydroxide)-bridged dimer.[11] Because the characterization of the oxidation product was not extensive and because it represents a structural type which is unique for manganese coordination chemistry, we felt this system was worthy of further investigation. The second system of interest involves [Mn(salpn)(H$_2$O)](ClO$_4$), a compound reported to evolve dioxygen when irradiated with visible light in the presence of *p*-benzoquinone.[12] Because mechanistic proposals for the evolution of dioxygen in this system involved dimer formation, we felt it would be useful to establish the structure of this compound. Herein we report the synthesis, structure, and magnetic and electrochemical behavior of [Mn(salpn)(EtOH)$_2$](ClO$_4$) (**1**) as well as that of the further oxidized bis(μ-oxo)dimanganese(IV) complex [Mn$_2$O$_2$(salpn)$_2$] (**2**), which has a remarkably low IV,IV/III,IV reduction potential.

Experimental Section

Methods. Infrared spectra were recorded on a Nicolet 5DX Fourier transform IR spectrometer with samples prepared as KBr pellets. UV–vis spectra were recorded on a Perkin-Elmer Lambda 9 UV/vis/near-IR spectrophotometer. NMR spectra were recorded on an in-house-modified Nicolet 250-MHz spectrometer. Solid-state magnetic susceptibilities were measured on a 800 VTS-50 SQUID magnetometer (SHE Corp.) in the temperature range 6–280 K at 5 kG. A correction for the susceptibility of the empty sample container was applied to the raw data, and diamagnetic corrections as estimated from Pascal's constants (**1**, 2.56×10^{-4} cgsu; **2**, 5.00×10^{-4} cgsu) were subtracted from the corrected data to obtain the molar susceptibilities. The resulting data were fit with the appropriate theoretical expression (see below) using a nonlinear least-squares refinement method.

[Mn(salpn)(H$_2$O)](ClO$_4$)·0.5H$_2$O (1). This compound was synthesized by a procedure similar to that of McAuliffe and co-workers.[12] A solution of 3.5 g (0.0125 mol) of the ligand salpn in 50 mL of methanol/ethanol (1:1) was treated with 0.5 g (0.0125 mol) of NaOH to form the monodeprotonated ligand. A 4.5-g (0.0125-mol) portion of Mn(ClO$_4$)$_2$·6H$_2$O was added to the resulting solution. Subsequent air oxidation, addition of diethyl ether, and filtration led to the isolation of **1** in 90% yield. Recrystallization was accomplished by cooling a saturated ethanol solution of **1** to 4 °C. Slow cooling of the reaction mixture prior to the addition of diethyl ether allows the isolation of crystals of [Mn(salpn)(EtOH)$_2$](ClO$_4$)·EtOH·H$_2$O (**1a**·EtOH·H$_2$O) suitable for X-ray diffraction studies (see below). IR data (cm^{-1}): 1612 (s), 1271 (s), 1124 (s), 623 (s), 454 (m), 379 (m). UV–vis data [λ, nm (ϵ, M^{-1} cm^{-1})], MeOH: 550 (420), 374 (9050), 278 (25 000). NMR data (CD$_3$CN; positions referenced against residual CHD$_2$CN, the proton resonance of which was taken to be at 1.93 ppm): 19.8 (2 H), 11.6 (4 H), 7.4 (2 H), −2.8 (2 H), −24.8 (2 H), −26.2 (2 H), −94.2 (2 H) ppm. μ_{eff}: 4.55 μ_B at 298 K. Elemental analysis was performed on a powdered sample of **1**. Anal. Calcd for C$_{17}$H$_{19}$N$_2$O$_{7.5}$MnCl: C, 44.22; H, 4.15; N, 6.07. Found: C, 44.47; H, 3.85; N, 6.10.

Table I. Summary of Crystal Data for [Mn(salpn)(EtOH)$_2$](ClO$_4$)·EtOH·H$_2$O (**1a**·EtOH·H$_2$O) and [Mn(salpn)O]$_2$·2DMF (**2**·2DMF)[a]

formula	$MnC_{23}H_{36}ClN_2O_{10}$	$MnC_{20}H_{23}N_4O_3$
mol wt	590.9	848.7
temp, °C	−125	−90
space group	$P\bar{1}$	$P2_1/c$
a, Å	11.649 (3)	10.772 (2)
b, Å	13.902 (6)	10.163 (3)
c, Å	19.849 (7)	17.564 (4)
α, deg	70.18 (2)	90.00
β, deg	70.52 (2)	100.67 (2)
γ, deg	60.33 (2)	90.00
V, Å^3	2726 (2)	1890 (1)
Z	4	2
ρ_{calcd}, g/cm^3	1.44	1.49
μ, cm^{-1}	6.167	7.01
λ, Å	0.71073	0.71073
2θ range, deg	3.0–45.0	4.0–55.0
no. of data used	5328 ($I \geq 3\sigma(I)$)	4174 ($\sigma\|F_o\| > 0$)
R	0.054	0.033
R_w	0.065	0.046

[a] Formulas used in structure solution: $R = \sum(|F_o| - |F_c|)/\sum|F_o|$; $R_w = [\sum w(|F_o| - |F_c|)^2/\sum w|F_o|^2]^{1/2}$; function minimized $\sum w(|F_o| - |F_c|)^2$; $w = 1/\sigma^2(|F_o|)$ ([Mn(salpn)(EtOH)$_2$](ClO$_4$)); $w = 1/\sigma^2(|F_o|) + 0.0008|F_o|^2$ ([Mn(salpn)O]$_2$).

[Mn(μ-O)(salpn)]$_2$ (2). Method 1. According to the procedure of Miller and Oliver,[10] 1.00 g (2.83 mmol) of Mn(salpn)(H$_2$O) was dissolved in a minimum of pyridine under an atmosphere of dinitrogen. The resulting orange solution was exposed to air, at which time it turned dark brown. This solution was stored at 3 °C for 1 week, and 0.73 g of a brown crystalline material was isolated by filtration. Recrystallization from methylene chloride/cyclohexane yielded crystals of **2**·CH$_2$Cl$_2$·C$_6$H$_{12}$ suitable for X-ray diffraction work.[13]

Method 2. Under nitrogen, a solution of 1.15 g (2.1 mmol) of **1** in methanol was treated with 0.087 g (2.1 mmol) of NaOH in methanol. The red-brown solid that precipitated was isolated by filtration and redissolved in DMF. Air oxidation of the resulting solution led to deposition of large hexagonal crystals of **2**·2DMF suitable for X-ray diffraction studies. The presence of a minor paramagnetic impurity necessiated that the material be recrystallized from hot (100 °C) DMF prior to carrying out magnetic measurements. Yield: 0.68 g, 77%. IR data (cm^{-1}): 1666 (s), 1624 (s), 1303 (s), 1262 (s), 645 (m), 614 (m), 450 (m). UV–vis data [λ, nm (ϵ, M^{-1} cm^{-1}], DMF: 670 sh (310), 470 sh (3500), 410 sh (4100), 320 sh (9300). Elemental analysis was performed on a powdered sample of **2**·2DMF·H$_2$O. Anal. Calcd for C$_{40}$H$_{48}$N$_6$O$_9$Mn$_2$: C, 55.43; H, 5.58; N, 9.70. Found: C, 55.33; H, 5.62; N, 9.71.

X-ray Structure Determination of [Mn(salpn)(EtOH)$_2$][ClO$_4$]·EtOH·H$_2$O (1a·EtOH·H$_2$O). Suitable crystals of **1a**·EtOH·H$_2$O were obtained by slow cooling of the reaction mixture. A solvent-loss-sensitive crystal of dimensions 0.40 × 0.40 × 0.30 mm was immersed in oil (Exxon Paratone-n), mounted on a glass fiber, and transferred to an Enraf-Nonius CAD-4 diffractometer equipped with a low-temperature unit. Cell parameters were obtained by least-squares refinement of the angular settings of 24 strong reflections in the range $23.4 < 2\theta < 27.6$. Low-temperature intensity data were collected using a θ–2θ scan technique with Mo Kα radiation under the conditions given in Table I. Three check reflections measured every 2 h of X-ray exposure showed no decay over the course of the data collection. The data were corrected for Lorentz and polarization effects. An empirical absorption correction based on ψ scans of three reflections at high χ angles was applied. The maximum and minimum transmission coefficients were 1.00 and 0.90, respectively. A Patterson map revealed the location of two manganese atoms per asymmetric unit, and all remaining non-hydrogen atoms were

(7) (a) George, G. N.; Prince, R. C.; Cramer, S. P. *Science* **1989**, *243*, 789. (b) Yachandra, V. K.; Guiles, R. D.; McDermott, A. E.; Cole, J. L.; Britt, R. D.; Dexheimer, S. L.; Sauer, K.; Klein, M. P. *Biochemistry* **1987**, *26*, 5974.
(8) Kipke, C. A.; Scott, M. J.; Gohdes, J. W.; Armstrong, W. H. *Inorg. Chem.* **1990**, *29*, 2197.
(9) Johnson, G. L.; Beveridge, W. D. *Inorg. Nucl. Chem. Lett.* **1967**, *3*, 323.
(10) Miller, J. D.; Oliver, D. *J. Inorg. Nucl. Chem.* **1972**, *34*, 1873.
(11) Malsen, H. S.; Waters, T. N. *J. Chem. Soc., Chem. Commun.* **1973**, 760.
(12) Ashmawy, F. M.; McAuliffe, C. A.; Parish, R. V.; Tames, J. *J. Chem. Soc., Dalton Trans.* **1985**, *1391*.
(13) X-ray analysis: Compound **2**·CH$_2$Cl$_2$·C$_6$H$_{12}$ crystallizes in the monoclinic space group $C2/c$ with a = 20.472 (5) Å, b = 8.817 (3) Å, c = 25.243 (5) Å, β = 111.49 (2)°, V = 4239 Å^3, and Z = 4. Data collection at 173 K in the range 2θ = 3–45° with Mo Kα radiation yielded 2810 reflections with $I \geq 3\sigma(I)$. The structure was solved by Patterson methods and refined using 280 parameters to final R (R_w) values of 4.6% (5.9%). The metrical parameters of the Mn complex in this crystal form are essentially identical to those reported here in full for the DMF solvate.

Table II. Atomic Coordinates and Equivalent Isotropic Thermal Parameters for $[Mn(salpn)(EtOH)_2](ClO_4)\cdot EtOH\cdot H_2O$ (**1a**·EtOH·H_2O)

atom	*x*	*y*	*z*	*B*,[a] Å²	atom	*x*	*y*	*z*	*B*,[a] Å²
Mn(1)	0.14999 (7)	0.37897 (5)	0.26268 (4)	2.21 (2)	C(8)	0.4765 (6)	0.5500 (5)	0.3757 (4)	5.4 (2)
Mn(2)	0.39349 (8)	0.84074 (6)	0.86273 (4)	2.90 (2)	C(9)	−0.0308 (7)	0.8910 (6)	0.3648 (5)	8.2 (3)
Cl(1)	−0.3141 (1)	0.7214 (1)	0.41671 (7)	3.33 (3)	C(10)	0.0120 (8)	0.8073 (7)	0.4328 (5)	9.0 (3)
Cl(2)	0.3194 (2)	0.8231 (1)	0.16769 (8)	4.91 (5)	C(11)	−0.0410 (5)	0.4652 (4)	0.1820 (3)	2.7 (1)
O(1)	0.0805 (3)	0.4119 (2)	0.1821 (2)	2.72 (9)	C(12)	−0.1025 (5)	0.4424 (4)	0.1424 (3)	4.2 (2)
O(2)	0.2316 (3)	0.2384 (2)	0.2499 (2)	2.40 (8)	C(13)	−0.2273 (6)	0.4976 (5)	0.1411 (3)	5.7 (2)
O(3)	0.3411 (3)	0.7285 (3)	0.9336 (2)	3.2 (1)	C(14)	−0.2961 (6)	0.5777 (5)	0.1778 (3)	5.2 (2)
O(4)	0.4623 (3)	0.7534 (2)	0.7947 (2)	2.78 (9)	C(15)	−0.2368 (5)	0.6025 (4)	0.2153 (3)	3.9 (2)
O(5)	−0.0183 (3)	0.3282 (2)	0.3405 (2)	2.67 (8)	C(16)	−0.1094 (5)	0.5467 (4)	0.2192 (3)	2.9 (1)
O(6)	0.3270 (3)	0.4228 (2)	0.1978 (2)	2.80 (9)	C(17)	−0.0501 (5)	0.5802 (4)	0.2561 (3)	2.9 (1)
O(7)	0.5877 (3)	0.7920 (3)	0.8810 (2)	3.5 (1)	C(21)	0.2358 (4)	0.1509 (4)	0.3055 (3)	2.5 (1)
O(8)	0.2062 (3)	0.9095 (3)	0.8311 (2)	3.6 (1)	C(22)	0.2356 (5)	0.0581 (4)	0.2941 (3)	3.1 (1)
O(9)	−0.3154 (4)	0.8069 (3)	0.4407 (2)	4.5 (1)	C(23)	0.2472 (5)	−0.0356 (4)	0.3490 (3)	3.6 (2)
O(10)	−0.1907 (4)	0.6443 (3)	0.4135 (2)	5.6 (1)	C(24)	0.2575 (5)	−0.0388 (4)	0.4168 (3)	3.6 (2)
O(11)	−0.3414 (4)	0.7603 (3)	0.3450 (2)	5.2 (1)	C(25)	0.2551 (5)	0.0536 (4)	0.4292 (3)	3.2 (1)
O(12)	−0.4064 (4)	0.6699 (3)	0.4687 (2)	5.6 (1)	C(26)	0.2433 (4)	0.1491 (4)	0.3747 (3)	2.4 (1)
O(13)	0.2480 (7)	0.8781 (5)	0.2216 (4)	7.2 (2)[b]	C(27)	0.2489 (4)	0.2404 (4)	0.3906 (3)	2.6 (1)
O(13′)	0.400 (1)	0.786 (1)	0.1087 (8)	7.5 (4)[c]	C(31)	0.2233 (5)	0.7419 (4)	0.9781 (3)	3.5 (2)
O(14)	0.2376 (8)	0.7800 (6)	0.1537 (4)	10.4 (3)[b]	C(32)	0.1642 (5)	0.6633 (5)	0.9970 (3)	4.0 (2)
O(14′)	0.208 (2)	0.791 (2)	0.180 (1)	11.0 (6)[c]	C(33)	0.0427 (6)	0.6761 (6)	1.0436 (3)	5.5 (2)
O(15)	0.3704 (9)	0.8942 (7)	0.1028 (4)	10.1 (3)[b]	C(34)	−0.0178 (6)	0.7651 (6)	1.0732 (4)	6.0 (2)
O(15′)	0.289 (1)	0.932 (1)	0.1447 (8)	7.4 (4)[c]	C(35)	0.0408 (6)	0.8406 (5)	1.0559 (3)	5.3 (2)
O(16)	0.424 (1)	0.7446 (7)	0.1951 (6)	12.9 (4)[b]	C(36)	0.1606 (5)	0.8326 (4)	1.0067 (3)	3.9 (2)
O(16′)	0.387 (1)	0.786 (1)	0.2223 (9)	7.9 (4)[c]	C(37)	0.2186 (6)	0.9131 (4)	0.9913 (3)	4.3 (2)
O(17)	0.3584 (4)	0.6725 (3)	0.4536 (2)	5.3 (1)	C(41)	0.4459 (4)	0.7885 (4)	0.7263 (3)	2.5 (1)
O(18)	0.0141 (7)	0.8479 (5)	0.3027 (4)	11.4 (2)	C(42)	0.4378 (5)	0.7170 (4)	0.6941 (3)	2.7 (1)
O(19)	0.1755 (4)	0.5797 (3)	0.5513 (2)	4.9 (1)	C(43)	0.4272 (5)	0.7494 (4)	0.6219 (3)	3.1 (1)
O(20)	0.1459 (7)	0.1191 (4)	0.7666 (3)	10.8 (2)	C(44)	0.4237 (5)	0.8525 (4)	0.5801 (3)	3.2 (1)
N(1)	0.0569 (4)	0.5290 (3)	0.2751 (2)	2.7 (1)	C(45)	0.4291 (5)	0.9239 (4)	0.6117 (3)	2.8 (1)
N(2)	0.2214 (3)	0.3373 (3)	0.3522 (2)	2.4 (1)	C(46)	0.4384 (4)	0.8940 (4)	0.6857 (3)	2.5 (1)
N(3)	0.3159 (5)	0.9286 (3)	0.9383 (2)	3.9 (1)	C(47)	0.4528 (5)	0.9700 (4)	0.7137 (3)	3.0 (1)
N(4)	0.4434 (4)	0.9631 (3)	0.7816 (2)	3.1 (1)	C(51)	−0.0813 (4)	0.2676 (4)	0.3279 (3)	3.2 (1)
C(1)	0.2467 (5)	0.4154 (4)	0.3756 (3)	3.2 (1)	C(52)	−0.1029 (5)	0.1779 (4)	0.3940 (3)	3.8 (2)
C(2)	0.1322 (5)	0.5137 (4)	0.3821 (3)	3.4 (1)	C(61)	0.3332 (6)	0.5064 (5)	0.1309 (4)	4.8 (2)
C(3)	0.1043 (5)	0.5821 (4)	0.3076 (3)	3.5 (1)	C(62)	0.4527 (6)	0.5296 (5)	0.1010 (4)	5.5 (2)
C(4)	0.4725 (6)	1.0461 (4)	0.7972 (3)	4.1 (2)	C(71)	0.6253 (6)	0.7429 (6)	0.9490 (3)	6.4 (2)
C(5)	0.3683 (7)	1.0934 (4)	0.8583 (3)	5.4 (2)	C(72)	0.7326 (8)	0.7613 (8)	0.9521 (4)	10.2 (3)
C(6)	0.3668 (7)	1.0140 (4)	0.9329 (3)	5.2 (2)	C(81)	0.1447 (5)	0.8537 (5)	0.8131 (3)	4.5 (2)
C(7)	0.3925 (6)	0.6600 (5)	0.3807 (4)	4.9 (2)	C(82)	0.0039 (6)	0.8784 (6)	0.8490 (4)	6.1 (2)

[a] The thermal parameter given for anisotropically refined atoms is the isotropic equivalent thermal parameter defined as $(4/3)[a^2B(1,1) + b^2B(2,2) + c^2B(3,3) + ab(\cos\gamma)B(1,2) + ac(\cos\beta)B(1,3) + bc(\cos\alpha)B(2,3)]$, where *a*, *b*, and *c* are real cell parameters and $B(i,j)$ are anisotropic β's. [b] Atoms were included at 0.67 site occupancy. [c] Atoms were included at 0.33 site occupancy with isotropic thermal parameters.

located by subsequent full-matrix least-squares refinement and difference Fourier methods using SDP software.

The complex crystallizes in the triclinic space group $P\bar{1}$, with two independent monomers per asymmetric unit. All hydrogen atoms except those bound to uncoordinated solvent molecules were located and placed in fixed calculated positions (C–H = 0.95 Å), and their positional as well as isotropic thermal parameters were constrained to "ride" on the atoms to which they are bound. All other atoms were refined with anisotropic thermal parameters with the exception of four oxygen atoms with partial occupancy in a disordered perchlorate anion. This anion displays a typical inversion disorder, with a 33%/66% occupany ratio of the two orientations. The final residual values were $R = 0.054$ and $R_w = 0.065$ based on 5328 independent data with $I \geq 3\sigma(I)$. The final difference Fourier map revealed considerable electron density in the region of the molecules of solvation with the largest peak being 0.98 e/Å. Attempts to improve the crystallographic model in this region of the lattice proved to be fruitless. The final values of the atomic positional parameters and their estimated standard deviations are provided in Table II. Hydrogen atom parameters as well as thermal parameters are available as supplementary material.

X-ray Structure Determination of $[Mn(\mu\text{-}O)(salpn)]_2\cdot 2DMF$ (2·2DMF). A dark red crystal of approximate dimensions 0.24 × 0.55 × 0.60 mm was immersed in oil, mounted on a glass fiber, and transferred to a Nicolet P3 diffractometer equipped with a modified LT-2 low-temperature system. Information regarding the structure determination is given in Table I. Three check reflections measured every 97 reflections showed no decay over the course of the data collection. The data were corrected for absorption and Lorentz and polarization effects. The structure was solved by direct methods (SHELXTL PLUS)[14] and refined by using full-matrix least-squares techniques.

(14) Nicolet Instrument Corp., Madison, WI, 1988.

The complex crystallizes in the monoclinic space group $P2_1/c$ with the molecule residing on an inversion center at 0, 0, $^1/_2$. All hydrogen atoms were located and included in the refinement with isotropic temperature factors. Refinement of positional and anisotropic thermal parameters for the remaining atoms led to convergence with $R = 0.033$ and $R_w = 0.046$ for 345 variables refined against all 4174 data with $|F_o| > 0$ ($R = 0.026$ and $R_w = 0.042$ for those 3644 data with $|F_o| > 6.0\sigma(|F_o|)$). A comparison of the thermal parameters of solvate and ligand atoms indicates full occupancy of the DMF lattice sites. The final values of the atomic positional parameters and their estimated standard deviations appear in Table III. Hydrogen atom parameters as well as thermal parameters are available as supplementary material.

Results and Discussion

The Mn(III) Monomer. A crystallographic study of **1a** was undertaken in order to establish if the manganese complex isolated from the reaction mixture of McAuliffe et al. is dimeric in the solid state as had been previously proposed.[12] Powdered samples of this product analyze well for the ethanol-free formulation $[Mn(salpn)(H_2O)](ClO_4)\cdot nH_2O$ ($n = 1, 1.5$).[12] At first inspection, the cell volume of **1a**·EtOH·H_2O appeared to be in harmony with a dimeric formulation. A full structure solution, however, revealed two independent, nearly identical monomers, with the closest Mn–Mn distance being 5.288 Å. An ORTEP view of one of the monomers appears in Figure 1. The ligand salpn binds with all four donors in the equatorial plane of the tetragonally distorted manganese coordination sphere, and the metal is only 0.033 Å out of the plane defined by the N_2O_2 donor set of the ligand. The axial positions are occupied by ethanol molecules, with one ethanol filling a partial pocket formed by the aromatic rings of the salpn phenolate groups. The Mn–O(EtOH) bond distances are elon-

Table III. Atomic Coordinates and Equivalent Isotropic Thermal Parameters for [Mn(salpn)O]$_2$·2DMF (**2**·2DMF)

atom	x	y	z	B,[a] Å^2
Mn(1)	−0.0052 (1)	0.1217 (1)	0.4668 (1)	1.10 (1)
O(1)	−0.1381 (1)	0.2502 (1)	0.4408 (1)	1.52 (2)
O(2)	0.1103 (1)	−0.0079 (1)	0.4968 (1)	1.30 (2)
O(3)	−0.0458 (1)	0.0624 (1)	0.3624 (1)	1.52 (2)
N(1)	0.0411 (1)	0.2166 (1)	0.5688 (1)	1.38 (3)
N(2)	0.1338 (1)	0.2365 (1)	0.4337 (1)	1.45 (3)
C(1)	−0.2131 (1)	0.2837 (1)	0.4890 (1)	1.48 (3)
C(2)	−0.3398 (2)	0.3173 (2)	0.4592 (1)	1.79 (4)
C(3)	−0.4197 (2)	0.3567 (2)	0.5079 (1)	2.08 (4)
C(4)	−0.3763 (2)	0.3693 (2)	0.5877 (1)	2.29 (5)
C(5)	−0.2527 (2)	0.3389 (2)	0.6183 (1)	2.06 (4)
C(6)	−0.1701 (2)	0.2940 (1)	0.5703 (1)	1.56 (3)
C(7)	−0.0389 (2)	0.2748 (2)	0.6031 (1)	1.56 (3)
C(8)	0.1755 (2)	0.2210 (2)	0.6030 (1)	1.80 (4)
C(9)	0.2442 (2)	0.3220 (2)	0.5604 (1)	2.53 (5)
C(10)	0.1754 (2)	0.3556 (2)	0.4789 (1)	1.99 (4)
C(11)	0.1913 (1)	0.2042 (2)	0.3787 (1)	1.65 (3)
C(12)	0.1570 (2)	0.0953 (2)	0.3263 (1)	1.63 (3)
C(13)	0.2410 (2)	0.0578 (2)	0.2773 (1)	2.08 (4)
C(14)	0.2103 (2)	−0.0414 (2)	0.2238 (1)	2.41 (4)
C(15)	0.0918 (2)	−0.1007 (2)	0.2148 (1)	2.31 (4)
C(16)	0.0062 (2)	−0.0636 (2)	0.2607 (1)	1.93 (4)
C(17)	0.0381 (1)	0.0325 (2)	0.3192 (1)	1.48 (3)
N(3)	0.4314 (1)	0.0328 (2)	0.6702 (1)	2.19 (3)
O(4)	0.4438 (2)	0.1598 (2)	0.7784 (1)	3.69 (4)
C(18)	0.4706 (2)	0.1362 (2)	0.7149 (1)	2.73 (5)
C(20)	0.3513 (2)	−0.0664 (2)	0.6954 (1)	2.81 (5)

[a] See footnote *a* of Table II.

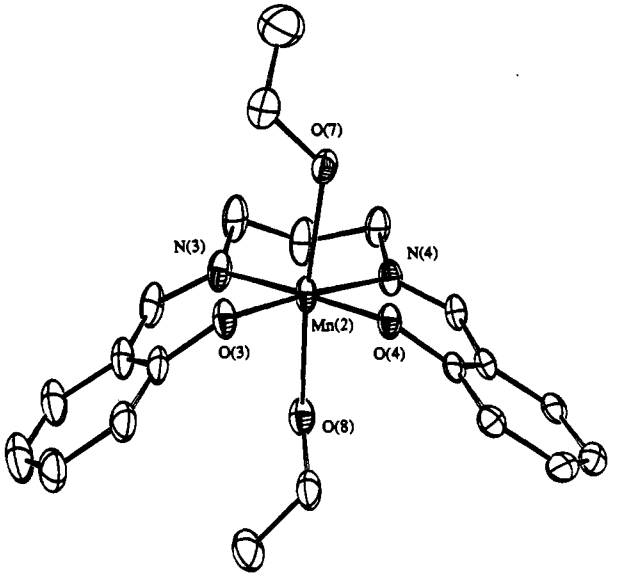

Figure 1. ORTEP representation of one monomer in structure of complex **1** at the 50% probability level.

gated due to a Jahn–Teller disortion at the d^4 metal center. Bond distances and angles within **1a** (Table IV) are unexceptional and comparable to those reported for other six-coordinate Mn^{III} Schiff base complexes.[15]

Ligation of water molecules to the manganese atom in six-coordinate Schiff base complexes has been demonstrated recently.[15] It was somewhat surprising to find ethanol rather than water bound to the manganese atom in **1a**, even though ample water is present in the reaction system that produces it and elemental analysis of powdered samples of **1** indicated that water rather than ethanol is present. This observation is consistent with samples of **1a** losing solvent when exposed to air with concomitant loss of crystallinity. It is not clear that the manganese complex remains monomeric with water replacing the ethanol in the axial coordination sites. The low magnetic moment observed for **1** indicates that dimer formation may occur in the solid state with solvent loss.

(15) Oki, A. R.; Hodgson, D. J. *Inorg. Chim. Acta* **1990**, *170*, 65.

Table IV. Interatomic Distances (Å) and Angles (deg) with Esd's for [Mn(salpn)(EtOH)$_2$](ClO$_4$)·EtOH·H$_2$O (**1a**·EtOH·H$_2$O)

Mn(1)–O(1)	1.874 (2)	Mn(2)–O(3)	1.855 (2)
Mn(1)–O(2)	1.891 (2)	Mn(2)–O(4)	1.900 (4)
Mn(1)–O(5)	2.235 (2)	Mn(2)–O(7)	2.219 (3)
Mn(1)–O(6)	2.215 (2)	Mn(2)–O(8)	2.235 (3)
Mn(1)–N(1)	2.017 (2)	Mn(2)–N(3)	2.019 (5)
Mn(1)–N(2)	2.028 (2)	Mn(2)–N(4)	2.022 (3)
O(1)–Mn(1)–O(2)	88.67 (9)	O(3)–Mn(2)–O(4)	88.4 (1)
O(1)–Mn(1)–O(5)	91.24 (8)	O(3)–Mn(2)–O(7)	97.0 (1)
O(1)–Mn(1)–O(6)	95.95 (8)	O(3)–Mn(2)–O(8)	91.4 (1)
O(1)–Mn(1)–N(1)	89.5 (1)	O(3)–Mn(2)–N(3)	89.0 (2)
O(1)–Mn(1)–N(2)	177.2 (1)	O(3)–Mn(2)–N(4)	176.3 (1)
O(2)–Mn(1)–O(5)	90.02 (8)	O(4)–Mn(2)–O(7)	87.9 (1)
O(2)–Mn(1)–O(6)	89.67 (8)	O(4)–Mn(2)–O(8)	92.0 (1)
O(2)–Mn(1)–N(1)	177.7 (1)	O(4)–Mn(2)–N(3)	177.3 (3)
O(2)–Mn(1)–N(2)	89.71 (9)	O(4)–Mn(2)–N(4)	89.7 (2)
O(5)–Mn(1)–O(6)	172.79 (8)	O(7)–Mn(2)–O(8)	171.59 (9)
O(5)–Mn(1)–N(1)	88.68 (9)	O(7)–Mn(2)–N(3)	93.0 (1)
O(5)–Mn(1)–N(2)	86.46 (9)	O(7)–Mn(2)–N(4)	86.2 (1)
O(6)–Mn(1)–N(1)	91.85 (9)	O(8)–Mn(2)–N(3)	87.4 (1)
O(6)–Mn(1)–N(2)	86.34 (9)	O(8)–Mn(2)–N(4)	85.4 (1)
N(1)–Mn(1)–N(2)	92.1 (1)	N(3)–Mn(2)–N(4)	92.8 (2)

In solution, solvent exchange at the axial sites in **1** is quite facile,[16] and its effects can be monitored in the electronic spectrum. As was noted previously,[12] in methanol this complex displays an absorption at 550 nm with a molar extinction coefficient of 410 M^{-1} cm^{-1}. It is reasonable to assign this band to a d–d transition for Mn(III) in a pseudotetragonal environment.[17] When the solvent is changed from methanol to acetonitrile, a charge-transfer band in the UV region shifts to lower energy and the transition at 550 nm becomes partially obscured. In more strongly coordinating solvents such as DMSO and DMF, this visible band appears only as a shoulder and is almost undetectable. The ^{1}H NMR spectrum of **1** in CD$_3$CN shows seven well resolved paramagnetically shifted peaks in the range +20 to −94 ppm. These peaks are assigned to the salpn ligand proton resonances, with axial solvent exchanging too rapidly to be observed. In a previous study of Mn(III) Schiff base complexes,[16a] the ^{1}H NMR spectral behavior of [Mn(salpn)(H$_2$O)](ClO$_4$) in MeOH-d_4 was examined and resonances at −22.6 and −25.0 ppm were assigned to the 4- and 5-positions of the ligand aromatic rings. When the solvent is changed to acetone-d_4, acetone-d_6/D$_2$O, or DMSO-d_6, the ^{1}H NMR spectrum remains essentially unchanged, indicating that the complex retains its structure under these varied solvent conditions. Thus the changes in the electronic spectra mentioned above are due to axial solvent exchange and/or to the varying dielectric nature of the media.

The Mn(IV) Dimer.[18] Although the aerobic oxidation of Mn(II) Schiff base complexes has been extensively studied, only two oxo- or hydroxo-bridged binuclear reaction products have been structurally characterized. The oxidation of [Mn(5-NO$_2$saldien)]$_2$, a binuclear manganese(II) complex of a pentadentate ligand, results in the formation of a complex with a mono(oxo)-bridged dimanganese (III) core.[8] Alternatively, the oxidation of Mn(salpn)(H$_2$O), a complex of a tetradentate Schiff base ligand, yields a compound that was assigned as a bis(hydroxo)-bridged dimanganese(III) species.[11] The current work reinvestigates this second oxidation product and demonstrates that it is correctly formulated as a bis(oxo)-bridged dimanganese(IV) compound (**2**).[10] Here we show that complex **2** can also be obtained by the oxidation of a trivalent manganese monomeric species under basic conditions.

(16) (a) Bonadies, J. A.; Maroney, M. J.; Pecoraro, V. L. *Inorg. Chem.* **1989**, *28*, 2044–2051. (b) Li, X.; Pecoraro, V. L. *Inorg. Chem.* **1989**, *28*, 3403.
(17) Lever, A. B. P. *Inorganic Electronic Spectroscopy*; Elsevier: Amsterdam, 1984; pp 440–444.
(18) Pecoraro and co-workers independently characterized **2**·2DMF by X-ray diffraction methods. See the following paper in this issue.

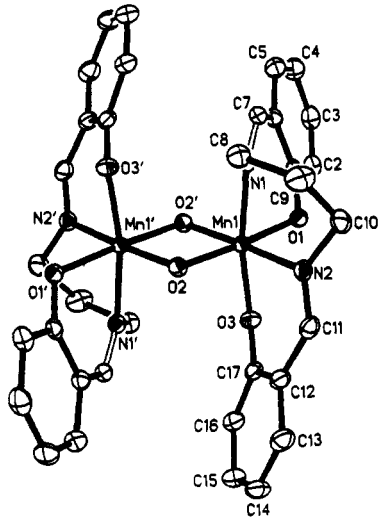

Figure 2. ORTEP representation of complex **2** at the 50% probability level. Primed and unprimed atoms are related by an inversion center.

Table V. Interatomic Distances (Å) and Angles (deg) with Esd's for $[Mn(salpn)O]_2 \cdot 2DMF$ (**2**·2DMF)

Mn(1)–O(2)	1.822 (1)	Mn(1)–O(2′)	1.816 (1)
Mn(1)–O(1)	1.929 (1)	Mn(1)–O(3)	1.903 (1)
Mn(1)–N(1)	2.013 (1)	Mn(1)–N(2)	2.065 (1)
Mn(1)–Mn(1′)	2.728 (1)		
Mn(1)–O(2)–Mn(1′)	97.2 (1)	O(2)–Mn(1)–O(2′)	82.8 (1)
O(1)–Mn(1)–O(2)	174.5 (1)	N(2)–Mn(1)–O(2′)	172.3 (1)
O(1)–Mn(1)–O(3)	87.6 (1)	O(1)–Mn(1)–N(2)	95.5 (1)
O(1)–Mn(1)–O(2′)	91.8 (1)	O(1)–Mn(1)–N(1)	86.4 (1)
O(2)–Mn(1)–N(1)	92.6 (1)	O(2)–Mn(1)–N(2)	89.9 (1)
O(3)–Mn(1)–N(2)	87.5 (1)	O(3)–Mn(1)–N(1)	169.7 (1)
O(3)–Mn(1)–N(2)	87.5 (1)	O(3)–Mn(1)–O(2′)	95.2 (1)
N(1)–Mn(1)–O(2′)	93.4 (1)	O(1)–Mn(1)–N(2)	84.7 (1)
Mn(1)–O(1)–C(1)	122.6 (1)	Mn(1)–O(3)–C(17)	124.7 (1)
Mn(1)–N(1)–C(7)	124.1 (1)	Mn(1)–N(1)–C(8)	116.3 (1)
Mn(1)–N(2)–C(10)	118.5 (1)	Mn(1)–N(2)–C(11)	123.0 (1)

An ORTEP plot of **2** is shown in Figure 2, and selected structural parameters appear in Table V. The molecule is situated on a crystallographically imposed inversion center. The structure consists of two Mn(IV) centers bridged by two O^{2-} ions to yield a planar Mn_2O_2 core with a Mn···Mn separation of 2.728 (1) Å. The ligand salpn donates two phenolic oxygen atoms and two imine nitrogen atoms to complete the roughly octahedral coordination environment around each manganese atom. Contrary to the equatorial binding mode of salpn observed for the structure of **1**, the ligand in **2** binds so as to leave two cis sites open for the bridging oxo groups. Adoption of this binding mode places one phenolic oxygen atom and one imine nitrogen atom trans to a bridging oxo group and one of each donor type in a cis position with respect to a bridging oxygen atom. A distinct lengthening of the bonds trans to the oxo groups is observed, with Mn–O distances of the cis and trans phenolate oxygen atoms being 1.903 (1) and 1.929 (1) Å, respectively, and the Mn–N distances of the cis and trans nitrogen atoms being 2.013 (1) and 2.065 (1) Å, respectively. Extensive structural comparisons of complexes with the $[Mn_2O_2]^{3+/4+}$ core have appeared recently,[19,20] and all structural parameters of **2** fall within the range noted previously. A more detailed discussion of these structural parameters as they pertain to the magnetic behavior of **2** follows.

Magnetic Susceptibility Studies. Variable-temperature, solid-state susceptibility measurements were made on powdered samples of **2** in the temperature range 5–280 K, and the results appear in Figure 3. The Mn atoms in the complex are antiferromagnetically coupled, with the effective magnetic moment per dimer decreasing monotonically from 2.64 μ_B at 280 K to 0.144 μ_B at 5 K. The data were fit by employing an expression derived from an isotropic spin-exchange Hamiltonian $\mathcal{H} = -2J\hat{S}_1 \cdot \hat{S}_2$ ($S_1 = S_2 = {}^3/_2$) and the Van Vleck equation.[21] Least-squares refinement yielded a satisfactory fit (not shown) with $J = -94$ cm^{-1}, TIP = 2.8×10^{-4}, $g = 2.0$ (fixed), and $P = 0.2\%$, where TIP is the temperature-independent paramagnetism and P is the mole percent of a paramagnetic impurity assumed to be a Mn(III) monomer. A substantially better fit (Figure 3) is obtained when the g value is also allowed to vary, and in this case, the parameters obtained are $J = -82$ cm^{-1}, $g = 1.79$, TIP = 2.8×10^{-4}, and $P = 0.1\%$.

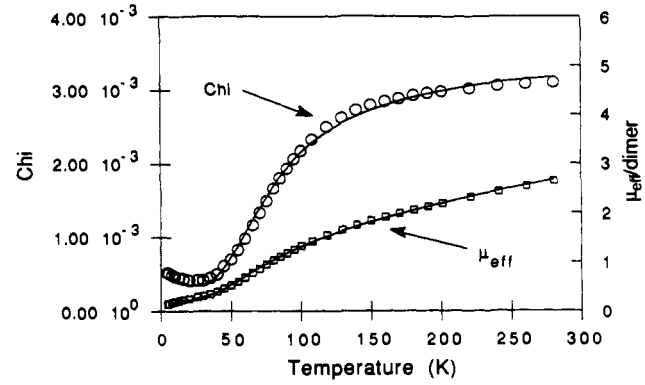

Figure 3. Plots of the molar susceptibility and effective magnetic moment per dimer vs temperature of a polycrystalline sample of complex **2**. Solid lines represent best fits of the data using the parameters described in the text.

The value of the magnetic exchange coupling constant for **2** is comparable to that reported recently for $[Mn_2O_2(pic)_4] \cdot MeCN$ (**3**), which has a J value of -87 cm^{-1}.[19] The J values for **2** and **3** are markedly lower than those reported for several other $\{Mn_2O_2\}^{4+}$ cores, which fall into the relatively narrow range of -127 to -150 cm^{-1}. Previously it was stated[19] that nothing in the metrical parameters of **3** compared to the only other structurally characterized examples of this core could be utilized to explain this anomalously low exchange value. The subsequent addition of $[Mn_2O_2(bispicen)_2](ClO_4)_4 \cdot 2CH_2CN$ (**4**)[20] as well as **2** to the growing set of species that contain the bis(oxo)-bridged dimanganese core does not allow one to make a more definitive statement in this regard. The Mn–O–Mn bond angle in **2** is 97.2 (1)°, which is intermediate between the angle in **4** of 95.1 (2)° and those in **3** and $[Mn_2O_2(phen)_4](ClO_4)_4$ (**5**),[21] which are 98.1 (2) and 99.5 (2)°, respectively. The average Mn–(μ-O) bond distance in **2** of 1.819 (1) Å is identical to the corresponding distance in **3**, 1.819 (3) Å, but it is slightly greater than the those in both **4** and **5**, which have average distances of 1.812 (3) and 1.801 (4) Å, respectively. The variation in Mn–(μ-O) bond distance follows the trend in J values, with larger bond distances correlating to weaker antiferromagnetic interactions. It was postulated that an increase in O-based peripheral ligation could cause an energy mismatch between the metal dπ orbitals and the pπ orbitals on the bridging oxo atoms which mediate the magnetic interaction.[19] The slight lengthening of the Mn–(μ-O) bond in **2** and **3** relative to **4** and **5** may be a consequence of somewhat weaker π bonding in the former cases.

Electrochemistry. A cyclic voltammogram of a DMSO solution of **1** shows one quasi-reversible reduction with an $E_{1/2}$ value of -0.154 V vs SSCE. This wave can be assigned as the $Mn^{III/II}$ redox couple and is consistent with values determined for other mononuclear Mn(III) Schiff base compounds.[16b,23] When this complex is oxidized in the presence of base, the bridging oxo groups of the species that forms (**2**) stabilize the higher oxidation states to a remarkable extent. This is made evident by inspection of the

(19) Libby, E.; Webb, R. J.; Streib, W. E.; Folting, K.; Huffman, J. C.; Hendrickson, D. N.; Christou, G. *Inorg. Chem.* **1989**, *28*, 4037.
(20) Goodson, P. A.; Glerup, J.; Hodgson, D. J.; Michelsen, K.; Pedersen, E. *Inorg. Chem.* **1990**, *29*, 503.
(21) O'Connor, C. J. *Prog. Inorg. Chem.* **1982**, *29*, 204.
(22) Stebler, M.; Ludi, A.; Bürgi, H.-B. *Inorg. Chem.* **1986**, *25*, 4743.
(23) Bogges, R. K.; Hughes, J. W.; Coleman, W. M.; Taylor, L. T. *Inorg. Chim. Acta* **1980**, *38*, 183.

cyclic voltammogram of 2 in DMSO, which reveals only one quasi-reversible reduction with an $E_{1/2}$ of -0.39V vs SSCE. This wave is assigned to the IV/IV, IV/III couple and is the lowest reduction potential for a $Mn^{IV}Mn^{IV}$ dimer reported. No other redox processes are accessible within the solvent window. This potential is more than 1 V more negative than the corresponding potential for 3 (0.66V vs SCE), even though the manganese atoms in both complexes have N_2O_4 donor sets. This is indicative of the remarkable ability of Schiff base ligands, particularly the phenolate donors, to stabilize high oxidation states. This result leads us to postulate that there are probably few phenolate donors to the Mn center in the PSII OEC, because a manganese aggregate with extensive phenolate ligation would not have a sufficiently high redox potential to carry out water oxidation.

Acknowledgment. This work was supported by Grant No. GM382751 from the National Institute of General Medical Sciences. W.H.A. is grateful for a Searle Scholars Award (1986-1989). We thank Dr. Joseph Ziller at the University of California at Irvine for performing the structural studies on compound 2.

Registry No. 1, 86773-55-9; 1a, 137596-42-0; 2, 51321-10-9; 2·2DMF, 137626-07-4; 2·2DMF·H_2O, 137626-06-3.

Supplementary Material Available: Listings of hydrogen atom parameters and anisotropic thermal parameters for 1 and 2 and a complete table of interatomic angles for 2 (7 pages); listings of observed and calculated structure amplitudes for 1 and 2 (57 pages). Ordering information is given on any current masthead page.

Contribution from the Department of Chemistry, University of Michigan, Ann Arbor, Michigan 48109-1055

Manganese-Manganese Separations in Oxide- and Alkoxide-Bridged Complexes: Correlation of Structure with Ligand Type and Number

Erlund Larson, Myoung Soo Lah, Xinhua Li, Joseph A. Bonadies, and Vincent L. Pecoraro*

Received August 17, 1990

Two dimeric manganese complexes have been prepared and their structures determined using X-ray crystallography. The first is a bis(μ_2-oxo) complex {$[Mn^{IV}(SALPN)O]_2$ (1), where SALPN = 1,3-bis(salicylideneamino)propane} which had previously been reported to be an Mn(III) dimer of composition $[Mn^{III}(SALPN)(OH)]_2$. Complex 1 can be prepared by hydrogen peroxide or air oxidation of a basic solution containing $Mn^{III}(SALPN)^+$ or by the reaction of Mn(SALPN)(acac) with hydrogen peroxide. In the latter reaction, isotopic labeling studies demonstrate that both μ_2-oxo atoms of 1 are derived from the same molecule of hydrogen peroxide. The second dimer is a bis(μ_2-alkoxo) complex {$[Mn^{III}(SALAHP)Cl(CH_3OH)]_2$ (2), where $H_2SALAHP$ = 1-(salicylideneamino)-3-hydroxypropane} which is the first example of a manganese dimer with unsupported alkoxide bridges and a rare example of a chloride-containing manganese dimer. These two new dimers and twenty other manganese complexes containing μ_2-oxo and μ_2-alkoxo groups are used to develop a correlation between manganese-manganese separation and Mn-O-Mn bridge angle. It is shown that complexes containing μ-oxo bridges conform to a law of cosines correlation between Mn-Mn separations and Mn-O-Mn bridge angles. In contrast, there is marked deviation from the law of cosines behavior when μ_2-alkoxo groups form the single-atom bridge. Surprisingly, an empirical correlation with a slope of 0.03 Å/deg over a 0.95-Å range (2.86-3.81 Å) and 33° angle deviation (96-129°) is observed. Structural implications are presented for established multinuclear manganese enzymes. Crystal data are as follows. 1: monoclinic, $P2_1/c$, a = 10.827 (4) Å, b = 10.241 (4) Å, c = 17.679 (7) Å, β = 100.07 (3)°, V = 1930 (1) Å^3, Z = 2; for 2434 data collected in the range $3 < 2\theta < 45°$ and 1787 data with $I > 2\sigma(I)$ the structure refined to R = 0.068 and R_w = 0.0434. 2: monoclinic, $P2_1/c$, a = 8.428 (3) Å, b = 12.966 (3) Å, c = 12.160 (3) Å, β = 109.58 (2)°, V = 1252 (1) Å^3, Z = 2; for 1562 data collected in the range $3 < 2\theta < 45°$ and 1229 data with $I > 3\sigma(I)$ the structure refined to R = 0.034 and R_w = 0.034.

Introduction

Manganese, often in the form of dimers or higher nuclearity aggregates, plays an important role in numerous biological processes associated with the utilization or generation of hydrogen peroxide or dioxygen. At least five functions of this type are known: manganese superoxide dismutase,[1,2] manganese catalase,[3-5] manganese peroxidase,[6] manganese ribonucleotide reductase,[7] and the oxygen-evolving complex (OEC).[8] At least three of these enzymes (catalases, ribonucleotides reductase, and the oxygen-evolving complex) contain active sites composed of two or more metals.

(1) Ludwig, M. L.; Pattridge, K. A.; Stallings, W. C. *Metabolism and Enzyme Function*; Academic Press: New York, 1986; p 405.
(2) Stallings, W. C.; Pattridge, K. A.; Strong, R. K.; Ludwig, M. L. *J. Biol. Chem.* **1985**, *260*, 16424.
(3) Beyer, W. F., Jr.; Frodovich, I. *Manganese in Metabolism and Enzyme Function*; Academic Press: New York, 1986; p 193.
(4) Khangulov, S. V.; Barynin, V. V.; Melik-Adamyin, V. R.; Grebenko, A. I.; Voevodskaya, N. V.; Blumenfeld, L. A.; Dobryakov, S. N.; Il'-Yasov, V. B. *Bioorg. Khim.* **1986**, *12*, 741. Fronko, R. M.; Penner-Hahn, J. E.; Bender, C. J. *J. Am. Chem. Soc.* **1988**, *110*, 7554.
(5) Allgood, G. S.; Perry, J. J. *J. Bacteriol.* **1986**, *168*, 563.
(6) Wariishi, H.; Akileswaran, L.; Gold, M. H. *Biochemistry* **1988**, *27*, 5365. Glenn, J. K.; Akileswaran, L.; Gold, M. H. *Arch. Biochem. Biophys.* **1986**, *251*, 688.
(7) Willing, A.; Follman, H.; Auling, G. *Eur. J. Biochem.* **1988**, *170*, 603.
(8) Recent reviews discussing these points: Pecoraro, V. L. *Photochem. Photobiol.* **1988**, *48*, 249. Babcock, G. T. *Photosynthesis*; Amesz, J., Ed.; New Comprehensive Biochemistry, Vol. 15; Elsevier: Amsterdam, 1987; p 125. Asmez, J. *Biochem. Biophys. Acta* **1983**, *726*, 1. Dismukes, G. C. *Photochem. Photobiol.* **1986**, *43*, 99. Babcock, G. T.; Barry, B. A.; Debus, R. J.; Hoganson, C. W.; Atamain, M.; McIntosh, L.; Sithole, I.; Yocum, C. F. *Biochemistry* **1989**, *28*, 9557. Rutherford, A. W. *Trends Biochem. Sci.* **1989**, *14*, 227. Ghanotakis, D. F.; Yocum, C. F. *Annu. Rev. Plant Physiol. Plant Mol. Biol.* **1990**, *41*, 274. Christou, G. *Acc. Chem. Res.* **1989**, *22*, 328. Wieghardt, K. *Angew. Chem., Int. Ed. Engl.* **1990**, *28*, 1153. Govindjee; Coleman, W. J. *Sci. Am.* **1990**, *262*, 50.

0020-1669/92/1331-0373$03.00/0